J Mater Sci (2008) 43:4512–4517
DOI 10.1007/s10853-008-2648-4

Determination of Young's moduli of 3C (110) single-crystal and (111) polycrystalline silicon carbide from operating frequencies

Wenteng Chang · Christian Zorman

Received: 3 February 2008 / Accepted: 11 April 2008 / Published online: 29 April 2008

Abstract This manuscript presents a Young's moduli analysis by folded-beam and straight-beam MEMS-based 3C silicon carbide (SiC) lateral resonators via finite element modeling. The modeling yields the ranges of the Young's modulus of (110) single-crystalline and (111) polycrystalline 3C–SiC resonators. This investigation considers the geometric variation of support beams as determined by scanning electron microscope (SEM) micrography. The Young's moduli of single-crystalline (110) and polycrystalline (111) 3C–SiC folded-beam resonators are estimated to be 337–386 GPa and 353–409 GPa by software modeling. The residual stress was 44 MPa for polycrystalline SiC. These results reveal that crystal orientation may be more important than crystallization in determining the Young's modulus of 3C–SiC.

Introduction

Microelectromechanical system (MEMS) resonators have attracted the attention of the radio frequency (RF) communications community because of their high quality factors (Q's) and their capacity for integration into silicon-based integrated circuits (IC) [1–3]. RF applications demand a device technology that operates from very low frequencies to ultra-high frequencies. Silicon carbide (SiC) is a promising material for RF MEMS because it has a high Young's modulus-to-density ratio, increasing the acoustic velocity and fundamental resonant frequency of the vibrating structure above those of Si. Among approximately 250 known polytypes of SiC, 3C–SiC (or β-SiC) is the only polytype that can be epitaxially grown as a single-crystal film on silicon substrates because it has a common crystal structure. Hence, 3C–SiC is the only suitable SiC for integration with current silicon-based technology. The Young's modulus of 3C–SiC has been obtained by a variety of methods, involving nanoindentation [4], quasi-static deflection [5], load deflection [6], the relationship between the resonant frequency and Young's modulus of a MEMS resonator [7], and a machined diaphragm [8]. The moduli of poly-SiC materials have been estimated to be from 300s to 700s GPa. The variation may arise from the polycrystalline characteristics, measurement techniques, and/or dimensions. This work employs the measured resonant frequencies of MEMS resonators—both poly-SiC and single-crystal SiC resonators—and addresses the variation of Young's modulus with geometric uncertainty associated with the fabrication process. A reasonable range of Young's modulus is explained by such fabrication uncertainty. The fabrication process critically affects geometric design, particularly of support beams, and thus determines a resonator's operating frequencies. Care must be taken to use resonant frequency to determine the Young's modulus of a material, because its value depends on its dimensions. Furthermore, a mechanical modeling is also helpful in determining the Young's modulus in addition to hand calculation.

W. Chang (✉)
Department of Electrical Engineering, National University of Kaohsiung, No. 700, Kaohsiung University Road, Nan-Tzu District, Kaohsiung 811, Taiwan
e-mail: wtchang@nuk.edu.tw

C. Zorman
Department of Electrical Engineering and Computer Science, Case Western Reserve University, 10900 Euclid Avenue, Cleveland, OH 44106, USA

Fabrication of resonators

The single-crystal 3C–SiC resonators used in this work were originally developed herein and called *Type K*. The fabrication sequence used the one-mask process to define the SiC resonators. In this design, the buried SiO_2 film of the silicon carbide-on-insulator wafers was used as a sacrificial layer and substrate electrical isolation. The fabrication process begins by depositing an aluminum thin film by magnetron sputtering. The aluminum film was patterned into an etch mask by photolithography, defining the resonator. The 3C–SiC film is anisotropically dry-etched using a reactive ion etching process that is based on CHF_3, O_2, and He. After the wafers were etched and diced, the chip level devices that contain resonators were then etched using an aluminum etchant and Piranha cleaning fluid to remove the aluminum mask. The structures were released by wet etching in 49% HF for 5 min (Fig. 1). *Type K* is shown in Fig. 2a [9].

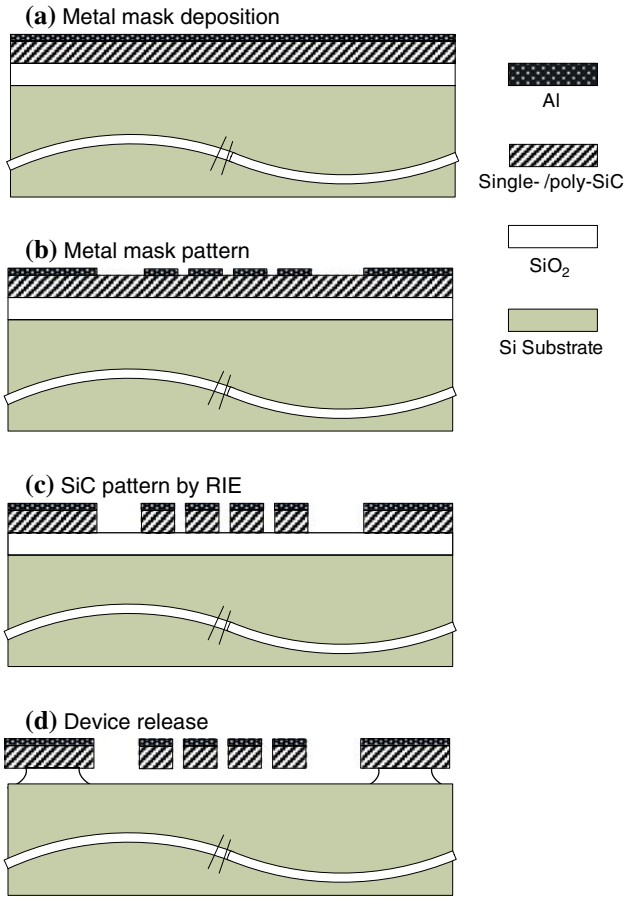

Fig. 1 Cross sections of the process flow for fabricating 3C–SiC lateral resonators herein; (**a**) deposition of SiO2/3C–SiC/Al; (**b**) mask patterning; (**c**) plasma etching of SiC structural material and etching mask removal; and (**d**) isotropic timed etching to release the device

Type D_f resonators shown in Fig. 2b were fabricated by poly-SiC films that were deposited by low pressure chemical vapor deposition (LPCVD). Dichlorosilane (DCS or SiH_2Cl_2) and acetylene (C_2H_2) were chosen as the resource gases because DCS is readily available and acetylene has a lower bond energy than propane, which makes it much more suitable for processes that must be performed at temperatures close to 900 °C. In many respects, the LPCVD furnace resembles the commercially available platforms that are commonly utilized for polysilicon MEMS. Details pertaining to the reactor and its use are presented elsewhere [10]. A series of resonators were fabricated from poly-SiC films that were deposited by LPCVD. The substrates comprised Si wafers that were capped with a thermally grown 2 μm-thick SiO_2 film. The poly-SiC films were simply deposited directly on top of the oxide surface without the need for preclean and carbonization steps, since the amorphous SiO_2 layer is not used as a template for film growth. The flow rates of DCS and C_2H_2 were 35 and 180 sccm, respectively. The C_2H_2 was diluted to 5% in hydrogen. The deposition pressure and temperature were fixed at 2 Torr and 900 °C throughout the process. Under these conditions the residual film stress was adjustable to near zero. To consider an optimal film quality, the residual stress was reported to be 44 MPa. The resistivity of a 1 μm-thick film was measured to be 3.38 Ω cm [11]. In addition to the folded-beam resonators, a series of straight-beam lateral resonators were also fabricated. The configuration of a straight-beam lateral resonator is shown in Fig. 2c. Like a folded-beam resonator, the straight-beam lateral resonator has comb fingers to maximize the capacitance between the shuttle and the drive and sense electrodes. The difference of *Type D_c* from *Type D_f* lies in the clamping architecture: the support beams are directly linked to the anchors, which presumably increases the clamping damping as compared with the folded-beam resonators. The resonator is denoted by *Type D_c* resonators also fabricated from poly-SiC films deposited using undoped LPCVD films.

Analysis and discussion

The natural resonant frequency of a folded-beam resonator has been derived from first principles using the law of energy conservation [12]. Simplifying the mass in the denominator by using an integral kinetic mass, M_I, enables the equation for the natural frequency of a folded-beam resonator to be rewritten as,

$$f_r = \frac{1}{2\pi}\left[\frac{2Eh(W/L)^3}{M_I}\right]^{1/2} \quad (1)$$

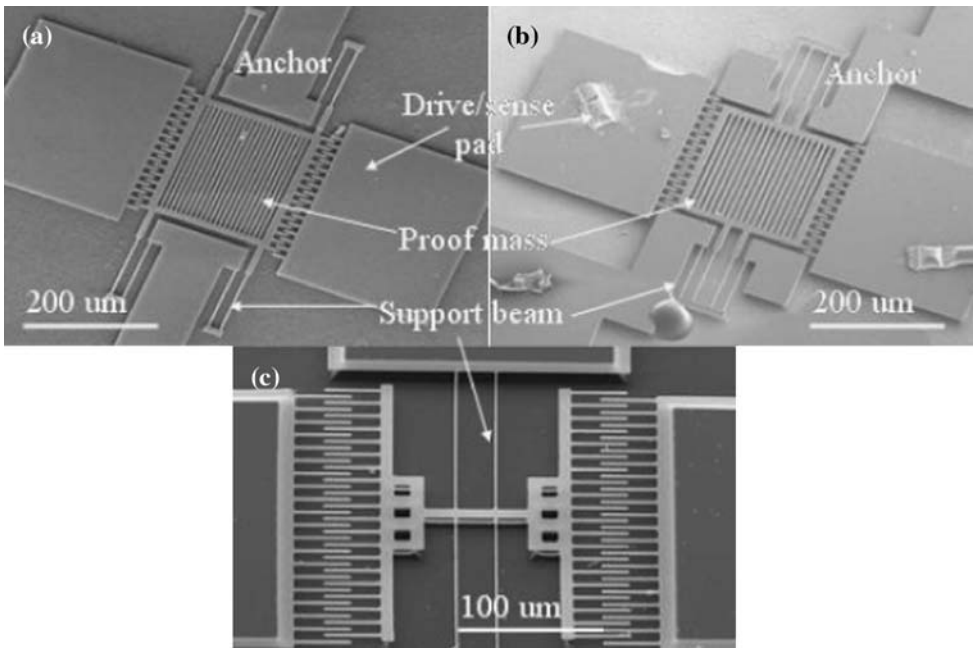

Fig. 2 Folded-beam resonators for *Type K* (**a**), *Type* D_f (**b**), and straight-beam resonators *Type* D_c (**c**)

where A_I denotes the integral kinetic area; ρ is the density of the material; E is the Young's modulus of the structural material for a folded-beam resonator; W and L are the width and length, respectively, of the support beam. The sensitivity of the measured dimensions W, L, and A_I to the resonant frequency can be evaluated from Eq. 2. The dimension sensitivity of resonant frequency (f_r) to the dimensions (D) of width (W), length (L), and effective area (A_I) are 3/2, 3/2, and 1/2. (D is replaced by W, L, and A_I).

$$\text{Dim. sensitivity} = \left|\frac{\partial f_r/f_r}{\partial D/D}\right| \tag{2}$$

The beam width (W) is more sensitive to desired resonant frequency than the other two (L and A_I) geometric features because of its small dimension and its uniformity of beam widths from one end to the other. So the values of Young's modulus calculated using these measurements have a high degree of uncertainty. Restated, the beam width is the most critical parameter in determining Young's modulus or resonant frequency. Figure 3a and b demonstrates the sidewalls of single-crystal and polycrystalline SiC resonators after the structures were released. The roughness of sidewalls is uniform on sidewall. In fact, these SiC resonators had columnar microstructures [13].

The measurement uses transmission method by Agilent 4395A network analyzer to acquire resonant frequency. The transmission signal S21 was directly read and detailed elsewhere [14]. The resonant frequencies for *Device K*1 and D_f1 are 28,162 and 45,081 Hz in Fig. 4a and b, respectively. The measured resonant frequency of *Device* D_c1 is 29,998 Hz in Fig. 4c.

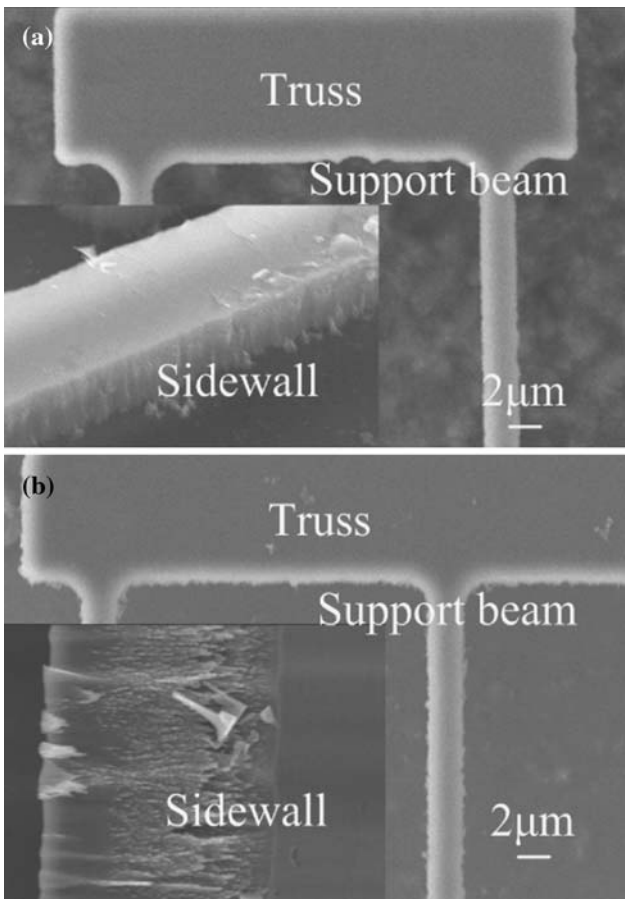

Fig. 3 The support beam and sidewall of single-crystal SiC (*Type K*) (**a**) and poly-SiC (*Type D*) (**b**) as rendered for analysis in this manuscript

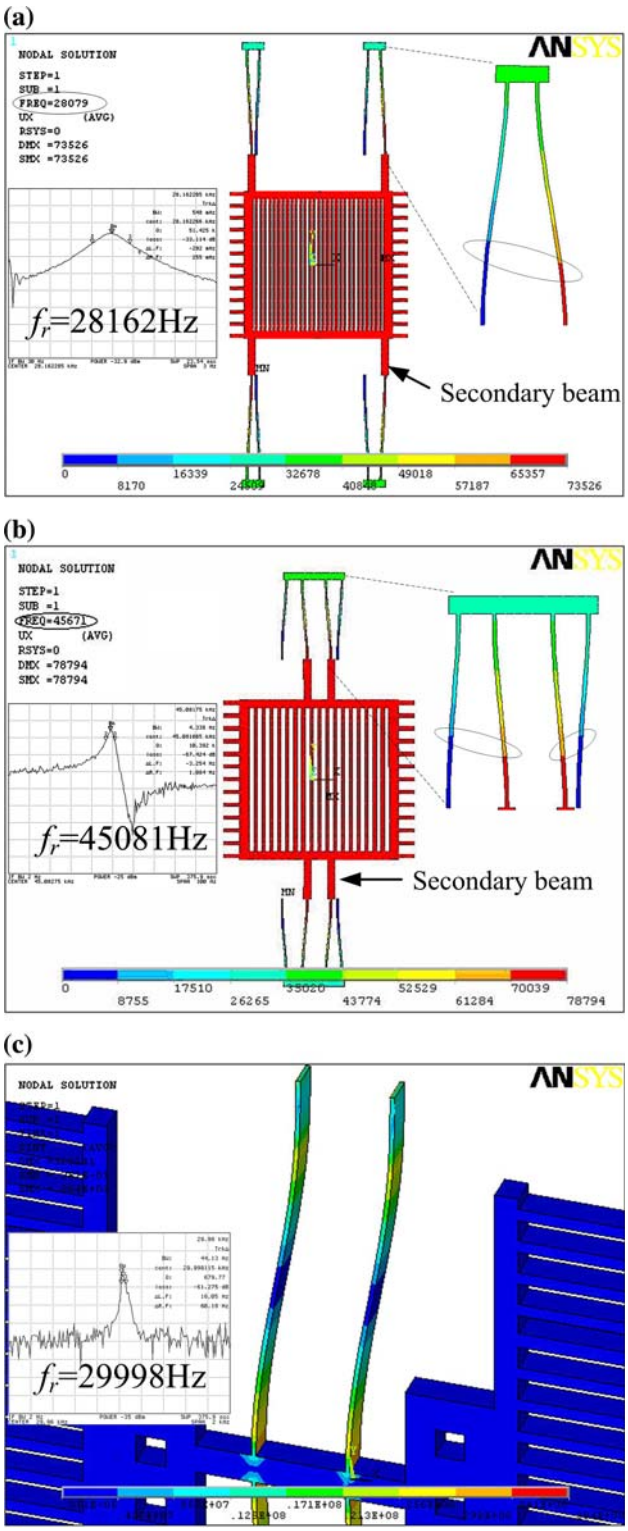

Fig. 4 Modeling of *Device K*1 in (**a**) D_f1 in (**b**), and D_c1 in (**c**). The colors represent the degree of physical displacement: the proof mass has the maximum displacement range, and is colored red; and the beam that is linked to the anchor has the minimum displacement and is blue. The displacements of two folded-beam resonators—with bonded truss (**a**) and separated truss (**b**)—are asymmetric because of the secondary beams in both cases: their secondary beams are parts of one of the folded beams. The resonant frequency measured from transmission method is determined to be 28,079 Hz for *Device K*1 and 45,081 Hz for *Device* D_f1and 29888 Hz for D_c1

The modeling by ANSYS verifies the values of Young's moduli. This modeling uses type Plane42, a 2D structural solid, with the thickness set at 2 μm. Table 1 includes the dimensions measured from SEM micrographs and the assumptions regarding SiC density and Poisson ratio as parameters for separated-truss and bonded-truss resonators. The *device K*1 is a separated-truss resonator that is fabricated from single-crystalline (110) 3C–SiC. The *device* D_f1 is a bonded-truss resonator that is fabricated from poly-crystalline (111) 3C–SiC. Subject to degree-of-freedom constraints on *X* and *Y* at the ends of the four support beams, the natural frequency can be obtained by finite element modeling. In this modeling effort, a range of Young's moduli are input to the model to determine the calculated resonant frequency that best matches the measured resonant frequency of *device K*1 and *device* D_f1 in Fig. 4a and b, respectively, which demonstrates the displacement of the movable structures, as indicated by the colors over a typical set of input values. Red represents the maximum displacement while blue represents the minimum. Note that the color-coded preliminary model in Fig. 4a and b indicates that the displacements of both bonded-truss and separated- truss folded-beams are asymmetric. The color codes in these two figures reveal that the support beams are not symmetrically located. The proof mass that represents maximum displacement range is red, and the beam that links to the anchor, representing the minimum displacement range, is blue. The displacements of the secondary beams are not completely stiff in this design, but rather, they act as a part of support beams that has some flexibility in the direction of motion. In this case, the width of the secondary beam is 10 μm, as determined from the SEM micrograph. The straight-beam resonator has no secondary beam problem. The modeling shows 34,460 Hz resonant frequency at 1.5 μm beam width.

The Young's moduli related to resonant frequency are also obtained by hand calculation. Based on energy conservation considerations that are only for a high Q device, such as these devices, the potential energy equals the total kinetic energy for all suspended parts of the resonator. Such a concept is expressed mathematically with the device deflected from center to either the right or the left, i.e., Fig. 4. The colors show the relative displacement of the movable components.

By energy conservation law,

Table 1 Dimensions, assumptions, hand calculation, and modeling results for *Device* $K1$, D_f1, and D_c1

Device		$K1$	D_f1	D_c1
Structural material		Single-crystal SiC	Poly-SiC	
Configuration		Folded-beam		Straight-beam
Dimensions	Beam width (m)	2.20×10^{-6}	2.05×10^{-6}	1.60×10^{-6}
	Beam length (m)	1.42×10^{-4}	1.00×10^{-4}	1.60×10^{-4}
	Proof mass area (m^2)	2.48×10^{-8}	2.37×10^{-8}	1.51×10^{-8}
	Truss area (m^2)	8.00×10^{-10}	6.93×10^{-10}	–
	Beam area (m^2)	2.5×10^{-9}	1.64×10^{-9}	9×10^{-10}
Assumption	Density (kg/m^3)	3.21×10^3	3.21×10^3	3.21×10^3
	Poisson ratio	0.23	0.17	0.17
Hand calculation	Young's modulus (Pa)	3.35×10^{11}	3.55×10^{11}	3.90×10^{11}
	Resonant frequency (Hz)	28,162	45,082	29,980
Modeling	Young's modulus (Pa)	3.60×10^{11}	3.80×10^{11}	4.10×10^{11}
	Resonant frequency (Hz)	28,079	45,671	30,060

$$\frac{1}{2}kX_0^2 = \frac{1}{2}M_S X_0^2\omega^2 + \frac{1}{2}M_t(cX_0\omega)^2 + \frac{13}{70}M_b(cX_0\omega)^2 + \frac{1}{4}M_b X_0^2\omega^2\left(1 - 3c + \frac{153}{35}c^2\right) \quad (3)$$

where

$$c = \frac{\text{truss displacement}}{\text{mass proof displacement}}, \quad 0 < c \leqq 0.5,$$

k is spring constant; M_S, M_t, and M_{b-f} represent the masses of the proof mass, the truss, and the support beam, respectively; X_0 is the maximum displacement of the proof mass; and ω is the angular speed in radians. The resonant frequency of a folded-beam resonator, f_{r_folded}, is shown in Eq. 4, where W_f and L_f are the width and length of the primary support beams; h is the thickness of the device; E is the Young's modulus. Hence, the resonant frequency of a folded-beam resonator can be rewritten as

$$f_{r\_folded} \cong \frac{1}{2\pi}\left[\frac{4cEh(W_f/L_f)^3}{(M_S + c^2M_t + 0.5(1 - 3c + 5.1c^2)M_{b-f}}\right]^{1/2} \quad (4)$$

Based on the modeling results for the separated-truss resonator in Fig. 4, the c for this device is estimated to be approximately 0.45 by making measurements of the deformation plot. Calculating the modified Young's modulus considering width variation of ±0.5 μm yields a value of 337–386 GPa for (110) single-crystal SiC and 353–409 GPa for (111) polycrystalline SiC. The range follows from the consideration of the support beam width as the only determinant of the value of the modulus because the beam width most strongly affects the estimated Young's modulus.

By the same method, the resonant frequency of a straight-beam resonator is estimated to be

$$f_{r\_straight} \cong \frac{1}{2\pi}\left[\frac{4Eh(W_c/L_c)^3}{M_S + 0.02M_{b-c}}\right]^{1/2} \quad (5)$$

where M_S is the proof mass; W_c and L_c are the width and length of the support beams; and M_{b-c} is the mass of the four support beams.

The results reveal that the orientation of 3C–SiC, rather than grain size, is probably more important in determining the Young's modulus. Notably, the finite element analysis makes many of the same basic assumptions as does the basic formula: the support beams have a low internal stress. Table 1 shows Young's moduli for both modeling and hand calculation. The modeling resonant frequency is determined to be 28,079 Hz at a Young's modulus of 360 GPa (a), and 45,671 Hz using a Young's modulus of 380 GPa (b) for folded-beam resonator. The hand calculation shows 6–7% lower than the modeling result. The hand calculation shows the Young's modulus of (111) polycrystalline SiC is to be about 430 GPa. This deviation is most likely attributed to the estimation of beam width.

Conclusion

The Young's moduli of single-crystalline (110) and polycrystalline (111) 3C–SiC folded-beam resonators were estimated to be 337–386 GPa and 353–409 GPa, using finite element modeling that considered the variation of support beam width due to fabrication uncertainties. The modeling yields the modification of a relationship between

the resonant frequency and the length of the support beams due to secondary support beams in these designs. These results reveal that crystal orientation may be more important than crystallization in determining the Young's modulus of 3C–SiC.

References

1. Nguyen CT-C, Howe RT (1999) IEEE J Solid-State Circuits 34:440
2. Gong JF, Xiao ZY, Chan PCH (2007) J Micromech Microeng 17:20
3. Uranga A, Teva J, Verd J, López JL, Torres F, Esteve J, Abadal G, Pérez-Murano F, Barniol N (2005) Electr Lett 41:1327
4. Sundararajan S, Bhushan B (1998) Wear 217:251
5. Serre C, Perez-Rodriguez A, Romano-Rodriguez A, Morante JR, Esteve J (1999) J Micromech Microeng 9:190
6. Fu X-A, Dunning J, Zorman CA, Mehregany M (2003) In: Proceedings of the 10th international conference on silicon carbide and related materials, ICSCRM 1519
7. Gao D, Wijesundara MBJ, Carraro C, Howe RT, Maboudian R (2003) Digest of technical papers. In: The 12th international conference on solid-state sensors and actuators, vol 2, p 1160
8. Roy S, Zorman CA, Mehregany M, DeAnna R, Deeb C (2006) J Appl Phys 99:44108
9. Kuo H-I, Zorman CA, Mehregany M (2003) Digest of technical papers. In: The 12th international conference on solid-state sensors and actuators, vol 1, p 742
10. Zorman CA, Rajgopal S, Fu XA, Jezeski R, Melzak J, Mehregany M (2002) Electrochem Solid-State Lett 5:99
11. Fu X-A, Dunning J, Zorman CA, Mehregany M (2005) Sens Actu A 119:169
12. Tang WC, Nguyen TCH, Howe RT (1989) Sens Actu A 20:25
13. Fu X-A, Jezeski R, Zorman CA, Mehregany M (2004) Appl Phys Lett 84:341
14. Chang W-T, Mehregany M, Zorman C (2007) In: Proceedings of the 2nd IEEE international conference on nano/micro engineered and molecular systems, p 740